Available online at www.sciencedirect.com

SciVerse ScienceDirect

Ceramics International 39 (2013) 1799–1806

CERAMICS INTERNATIONAL

www.elsevier.com/locate/ceramint

Deposition of the low resistive Ag–N dual acceptor doped p-type ZnO thin films

R. Swapna, M.C. Santhosh Kumar*

Advanced Materials Laboratory, Department of Physics, National Institute of Technology, Tiruchirappalli 620015, India

Received 17 June 2012; received in revised form 2 August 2012; accepted 3 August 2012
Available online 24 August 2012

Abstract

Nanocrystalline Ag and N dual-acceptor doped zinc oxide (ZnO:(Ag, N)) films were deposited on glass substrates by the spray pyrolysis technique. The Hall measurement, X-ray diffraction (XRD), scanning electron microscopy (SEM), energy dispersive X-ray spectroscopy (EDX), UV–vis and luminescence spectroscopy techniques were employed to investigate the electrical, structural, morphological and optical properties of the films in detail as a function of concentration of dopants. The atomic force microscopy (AFM) technique was employed to study the surface roughness and 3D surface profiles of the films. The Hall measurement results showed that all the ZnO:(Ag, N) films exhibited p-type conduction. The films with a doping concentration of 4 at% is found to show the lowest resistivity of $8.70 \times 10^{-2}\ \Omega$ cm and highest carrier concentration of $2.17 \times 10^{18}\ \mathrm{cm}^{-3}$. The XRD results revealed that all the films have good crystalline quality with a preferential *c*-axis orientation. The SEM micrographs of all the films exhibited uniformly distributed spherical grains over the surface of the films. The EDX and elemental mapping results showed the presence and distribution of Zn, O, Ag and N in the deposited films. The as-deposited ZnO:(Ag, N) films showed an average transmittance of about 90% in the visible region. The photoluminescence (PL) results suggested the suppression of native defect levels due to the incorporation of Ag and N in to the ZnO films.

Keywords: A. Films; B. Grain size; C. Electrical properties; D. ZnO

1. Introduction

In recent years ZnO has become a promising material for solar cells, surface acoustic wave devices [1], optoelectronic devices such as ultraviolet light-emitting diodes, laser diodes and photodetectors [2]. Among the available wide band gap semiconductors, ZnO is considered as the brightest emitter even at room temperature as it has wide band gap (3.37 eV) and large excitation binding energy (60 meV) [3]. Recent reports on the p-type conductivity in ZnO are broadening the scope for homo- and heterojunction ZnO devices. For the development of ZnO based devices, it is necessary to have p-type and n-type ZnO [4]. First principles total energy calculations showed that the oxygen vacancy (V_O) and zinc interstitial (Zn_i) defects in ZnO have low formation energies and these intrinsic defects act as the sources for the unintentional n-type conductivity [5]. Hence, achieving p-type conduction in ZnO is difficult due to the self-compensation effect and low solubility of the acceptor dopants in ZnO [6]. There are many reports claiming the realization of p-type conduction in ZnO films by mono-doping of group V elements such as N [7,8], P [9,10], As [10,11] and Sb [12], or group I elements like Ag [13] and Li [14]. Recently, a dual-doping method using two acceptor agents namely Li–N [15,16] or As–N [17] was proposed to prepare p-type ZnO. In this line, Zhang et al. [18] suggested that the dual-doping method is the best channel to overcome the difficulties in achieving p-type ZnO.

Furthermore, reproducible and long-time stable p-type ZnO has been realized by the dual-acceptor doping of silver and nitrogen. Ag and N are the two best candidates for producing p-type ZnO considering the strain effects

*Corresponding author. Tel.: +91 431 2503611; fax: +91 431 2500133.
E-mail addresses: swapna.ramella@yahoo.com (R. Swapna), santhoshmc@nitt.edu, santhoshmc@yahoo.com (M.C. Santhosh Kumar).

0272-8842/$ - see front matter © 2012 Elsevier Ltd and Techna Group S.r.l. All rights reserved.
http://dx.doi.org/10.1016/j.ceramint.2012.08.027

and energy levels of substitutional Ag_{Zn} and N_O acceptors. However, there are only a few studies on ZnO:(Ag, N) films reported in literature. Recently, Yan et al. [4] reported the fabrication of p-type ZnO:(Ag, N) films with good electrical properties by ion beam assisted deposition. Similarly, Bin et al. [19] fabricated the p-type ZnO films by dual-acceptor doping of Ag and N using the ultrasonic spray pyrolysis technique. In the present study, p-type ZnO:(Ag, N) films with low resistivity were achieved by spray pyrolysis. The spray pyrolysis technique is a simple, economical and more versatile than other chemical deposition techniques. In addition, it allows the possibility of obtaining films with the required properties for different applications. Further, it can be easily adapted for the production of large-area films [20]. In this paper, the authors concentrate on the effect of doping concentrations of Ag and N on the structural, morphological, compositional, electrical transport and optical properties of ZnO films deposited by the spray pyrolysis technique.

2. Experimental

In the present work the ZnO:(Ag, N) films were deposited using a spray solution mainly comprises of 0.1 M $Zn(CH_3COO)_2 \cdot 2H_2O$ (Sigma-Aldrich, 99.5%, Germany) dissolved in a mixture of deionized water and ethanol (Merck, 99.9%, Germany) taken in the proportion of 9:1 respectively. The dopant concentration was varied from 0 to 4 at% for both Ag and N. The Ag and N dual doping was achieved by dissolving an appropriate quantity of $AgNO_3$ (Sigma-Aldrich, 99.9%, USA) and $CH_3 \cdot COONH_4$ (Sigma-Aldrich, 99.9%, Germany) in the zinc acetate solution. A small amount of acetic acid (Merck, 99.9%, Germany) was added into the spray solution to avoid the formation of hydroxides [21]. The ZnO:(Ag, N) films were deposited on glass substrates by spray pyrolysis at a substrate temperature of 623 K. Prior to the film deposition, the glass substrates were cleaned with detergent solution and deionized water. Further, ultrasonic cleaning was carried out for 30 min in an ultrasonic bath and then rinsed in acetone for 10 min. The distance between the spray nozzle and the substrate was maintained at about 10 cm. The prepared solution is sprayed (3 ml/min) onto the clean glass substrates for a deposition time of 3 min. In this procedure, compressed air was used to atomize the solution containing the precursor compounds through a spray nozzle over the heated substrate. The precursor is pyrolyzed on the heated substrate where the pyrolytic decomposition process occurs and high quality ZnO:(Ag, N) films were produced with an average thickness of 987 nm.

The structural properties of the deposited ZnO:(Ag, N) films were investigated by X-ray diffraction (XRD) measurements using a Rigaku D/Max ULTIMA III diffractometer with CuK_α radiation ($\lambda = 1.5406$ Å). The thickness was measured using stylus profile meter. The surface morphology and the compositional analysis of the films were carried out by a scanning electron microscope (S3000N, Hitachi) equipped with energy dispersive X-ray spectroscopy and elemental mapping facilities. Atomic force microscopy (NTMDT-NTEGRA, Russia) was employed to analyze the surface roughness of the films. The optical measurements of undoped and ZnO:(Ag, N) films were carried out at room temperature using a Shimadzu UV-1700 spectrophotometer in the wavelength range of 300–1100 nm. Photoluminescence spectra were recorded at room temperature using Perkin Elmer LS 55 luminescence spectrophotometer with an excitation wavelength of 325 nm. Electrical resistivity, carrier concentration and mobility were measured at room temperature using an Ecopia Hall measurement system (Model: HMS-5000) in the van der Pauw configuration.

3. Results and discussion

3.1. Structural analysis

Fig. 1 shows the XRD patterns of ZnO:(Ag, N) thin films with Ag and N dopants concentration varied from 0 at% to 4 at%. It can be observed from Fig. 1 that all the films exhibit the characteristic diffraction peaks of ZnO (JCPDS card: 75-0576) indicating that the films are in polycrystalline form with wurtzite structure. Further, no characteristic peaks corresponding to the presence of secondary phases are observed implying that the dopants have not destroyed the ZnO structure and act as typical dopants. A switching in the preferential growth from the (100) plane to the (002) plane is observed when the dopant concentration increases from 1 to 4 at%. Generally, the direction with the highest planar density of lattice points corresponds to the lowest surface free energy which facilitates an easier grain growth in that direction [22]. The change in the preferential growth from the (100) plane to (002) plane observed in all the ZnO:(Ag, N) films

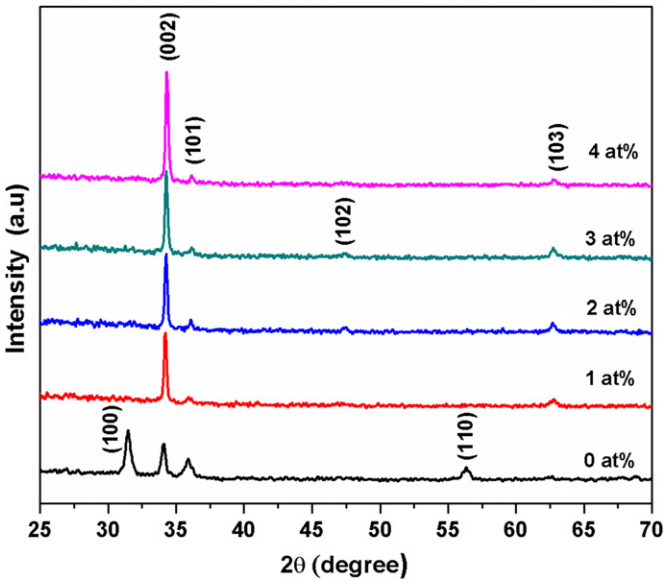

Fig. 1. XRD spectra of ZnO:(Ag, N) thin films.

suggests that the incorporation of Ag and N in to ZnO enhances the grain growth by decreasing the surface free energy in the (002) direction. As a result, all the ZnO:(Ag, N) films show a strong and narrow (002) diffraction peak indicating that the films have preferential *c*-axis orientation in the (002) direction. Similarly, Fujimura et al. [23] also reported that sputtered ZnO thin films were generally polycrystalline with a *c*-axis preferential orientation due to the lowest surface free energy of the (002) plane in ZnO. It can also be observed from Fig. 1 that the intensity of the (002) peak increases gradually and reaches the maximum at a dopant concentration of 4 at% for both Ag and N. But, the other diffraction planes show a low intensity in the films. The average crystallite size '*D*' is calculated using Scherrer's formula [24]

$$D = \frac{k\lambda}{\beta \cos\theta} \quad (1)$$

where λ is the wavelength of CuK_α radiation (1.5406 Å), k is the shape factor (0.9), β is the instrumental corrected full-width at the half-maximum (FWHM) intensity and θ is Bragg's diffraction angle. Fig. 2(a) shows the variation in average crystallite size with dopant concentration. The crystallite size increases with increase of dopant concentration.

The preferential or random growth of polycrystalline thin films can be understood by calculating the texture coefficient TC(*hkl*) for all the planes. The texture coefficient TC(*hkl*) is calculated for the characteristic diffraction planes from the X-ray diffraction data using the well-known formula [20]

$$TC(hkl) = \left(\frac{I_{(hkl)}/I_{o(hkl)}}{(1/N)\sum I_{(hkl)}/I_{o(hkl)}} \right) \quad (2)$$

where $I_{(hkl)}$ indicates the X-ray diffraction intensity obtained from the films and N is the number of reflections observed in the XRD pattern. $I_{o(hkl)}$ is the intensity of the standard diffraction pattern (JCPDS card: 75-0576). The texture coefficient (TC) represents the texture of the particular plane, deviation of which from unity implies the preferred growth. The value of the texture coefficient indicates the maximum preferred orientation of the films along the diffraction plane, meaning that the increase in preferred orientation is associated with increase in the number of grains along that plane. The texture coefficient calculated for the three main diffraction peaks namely (002), (110) and (103) are presented in Fig. 2(b). It can be seen that the highest TC is obtained for (002) plane in all the films. As seen in this figure, the TC(*hkl*) values for the other two peaks are almost below 1, indicating that the ZnO:(Ag, N) films do not exhibit preferred orientation along (110) and (103). The texture coefficients of the (002) plane of the films are between 1.64 and 3.37. The increasing texture coefficient causes the increase in the crystallite size of the films. It means that crystalline quality has been improved upon ZnO:(Ag, N) dual doping.

3.2. Surface morphology studies

Fig. 3(a)–(e) shows the SEM surface micrographs of ZnO:(Ag, N) films with different dopant concentrations from 0 at% to 4 at%. The microstructure of all the films consists of many spherical grains distributed regularly throughout the film surface. There are no visible pores and defects over the film surfaces. It can be observed from Fig. 3 that the grain size of the ZnO:(Ag, N) films increases as the Ag and N concentration is increased to 4 at%. In addition, light colored nanograins distributing in the dark matrix can be observed in Fig. 3(b)–(e). Fig. 4 illustrates the EDX spectrum and elemental mapping results showing the presence and distribution of Zn, O, Ag and N for the 4 at% Ag and N doped ZnO films. It can be observed from Fig. 4 that the composition of the prepared film constitutes Zn, O, Ag and N that are distributed regularly over the film surface and no significant signal distribution corresponding to secondary phase formation was observed. This result suggests that the observed

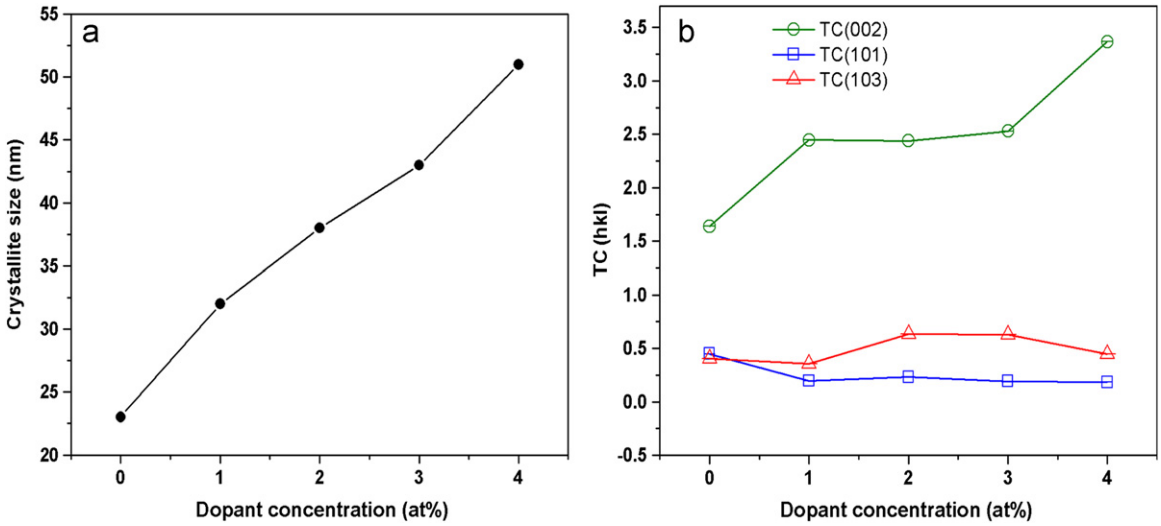

Fig. 2. (a) Variation of crystallite size (b) variation of TC(002), TC(101) and TC(103) as a function of (Ag, N) concentration.

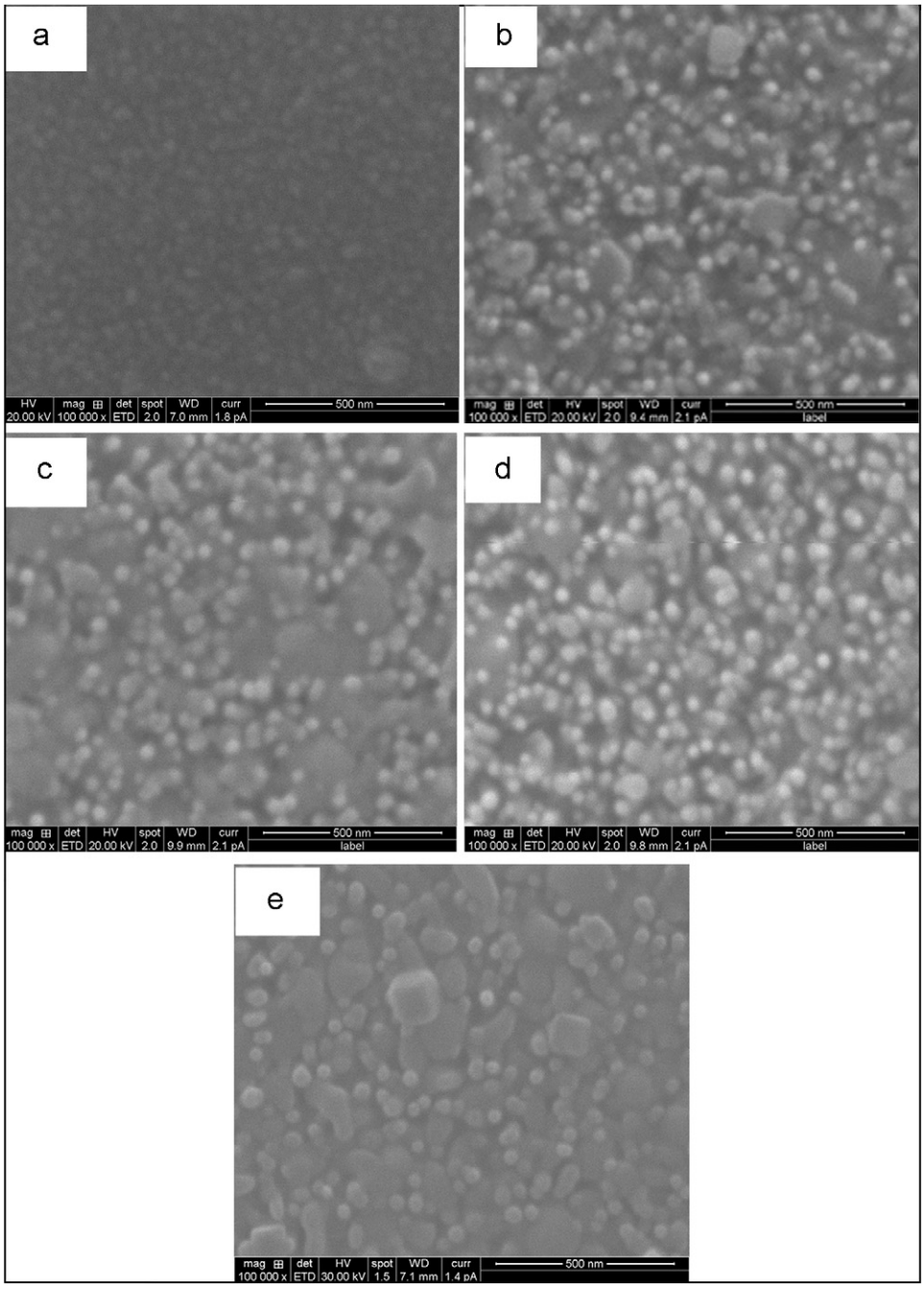

Fig. 3. SEM images of the ZnO:(Ag, N) films with (a) 0 at%, (b) 1 at%, (c) 2 at%, (d) 3 at% and (e) 4 at%.

light-colored nanograins distributing in the dark matrix material in the SEM images [Fig. 3 (b)–(e)] may not correspond to the secondary phase formation or segregation. Hence, the appearance of light colored grains may be attributed to the variation in the contrast of the secondary electron signal coming from suitably oriented ZnO grains. Similar kind of light colored nanograin distribution in the SEM images can also be observed in the reports published by Yan et al. [4]. The chemical compositions of Zn, N, Ag, and O in the ZnO:(Ag, N) films have been determined as 30.30, 2.33, 0.61 and 66.76 at%, respectively.

Fig. 5(a) and (b) shows the 3D AFM images of the ZnO:(Ag, N) films observed at 1 at% and 4 at% dopant concentrations respectively. The AFM images were recorded over a scan area of 1 μm × 1 μm. The RMS roughness of the films with a lower doping concentration of 1 at% is 9.77 nm and that with a higher value of 4 at% doping levels is 15.45 nm. This indicates that the increase in dopant concentration tend to increase the particle size and the surface roughness. The particle size is found to increase from 94 nm to 131 nm with the increase of dopant concentration from 0 to 4 at%. The size of the particle

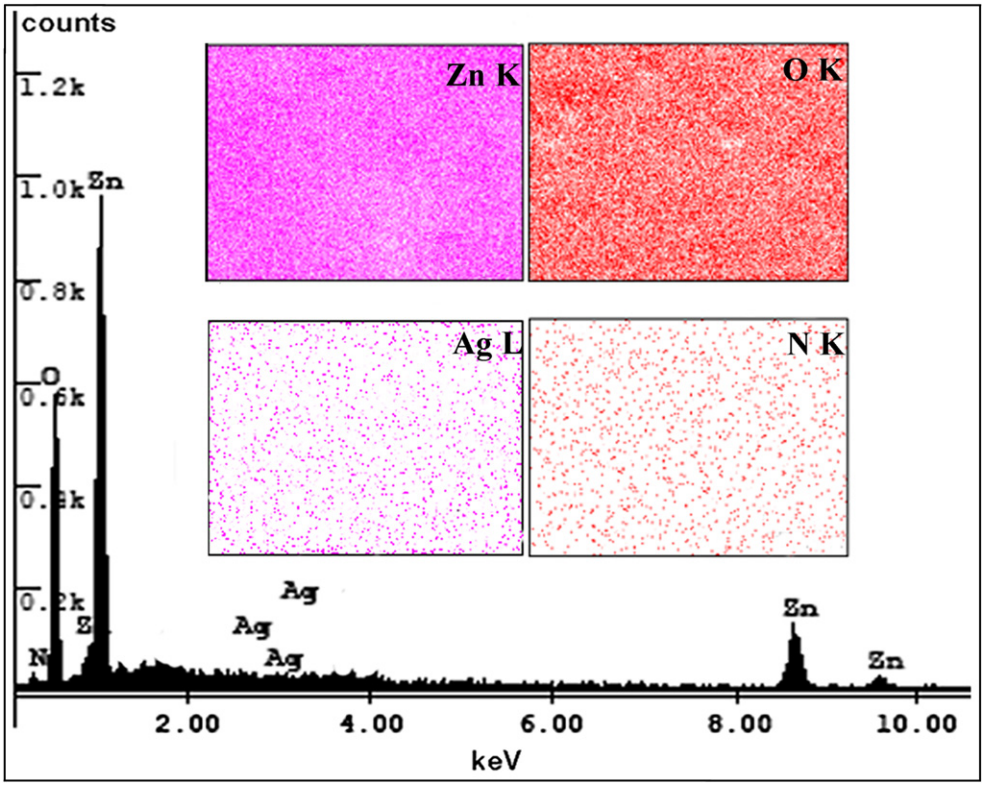

Fig.4. EDX and elemental mapping results showing for 4 at% ZnO:(Ag, N) films.

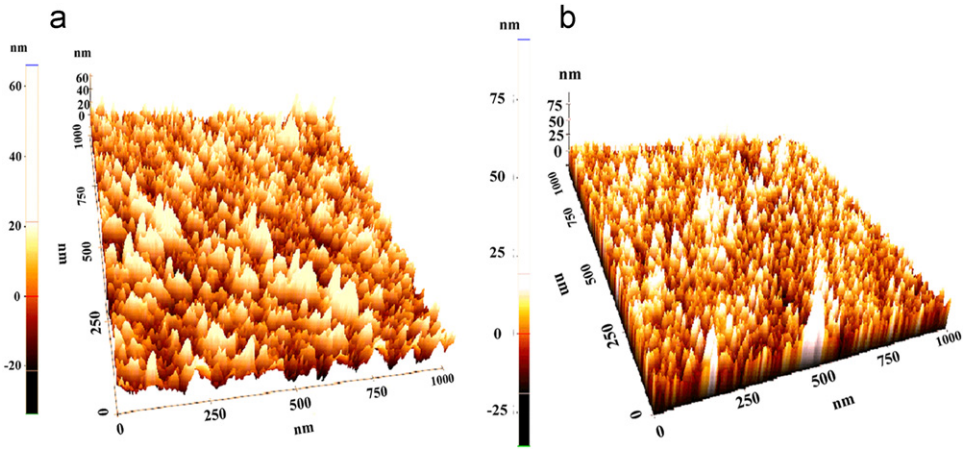

Fig. 5. AFM 3D images of the ZnO:(Ag, N) films with (a) 1 at% and (b) 4 at%.

measured from the AFM surface micrograph is higher than the values calculated from the XRD studies, indicating that these particles are probably an aggregation of small crystallites on the surface of the films.

3.3. Electrical studies

The Hall measurement technique is employed to measure the electrical properties and to determine the nature (p-type or n-type) of conduction in the ZnO:(Ag, N) films. Table 1 shows the measured electrical resistivity, corresponding carrier concentration and mobility of ZnO:(Ag, N) films of various dopant concentrations. It can be observed from Table 1 that the undoped ZnO film shows n-type conductivity due to the native donor defects such as zinc interstitial (Zn_i) and oxygen vacancy (V_O). Furthermore, the undoped ZnO film shows high resistivity of $3.33 \times 10^3\ \Omega\,cm$ with a carrier concentration of $5.65 \times 10^{15}\ cm^{-3}$ compared to that of ZnO:(Ag, N) films. Hence, the electrical study results of undoped ZnO film suggest that the above mentioned intrinsic defects need to be suppressed for the fabrication of p-type ZnO films [25].

Table 1
Variation of electrical resistivity (ρ), carrier concentration (n) and mobility (μ) of the ZnO:(Ag, N) films with dopant concentration.

Concentration (at%) Ag:N	Resistivity (Ω cm)	Carrier concentration (cm^{-3})	Mobility ($cm^2 V^{-1} s^{-1}$)	Carrier type
0:0	3.33×10^3	5.65×10^{15}	0.334	n
1:1	17.4	1.01×10^{17}	3.55	p
2:2	0.569	5.23×10^{17}	21.1	p
3:3	0.168	8.10×10^{17}	45.6	p
4:4	0.087	2.17×10^{18}	33.0	p

Table 2
Carrier concentrations as a function of the preservation period after deposition of ZnO:(Ag, N) films with dopant concentration.

Concentration (at%)Ag:N	As-prepared n_0 (cm^{-3})	After 3 months n_3 (cm^{-3})	After 6 months n_6 (cm^{-3})	Carrier type
1:1	1.01×10^{17}	9.96×10^{16}	8.71×10^{16}	p
2:2	5.23×10^{17}	4.84×10^{17}	3.90×10^{17}	p
3:3	8.10×10^{17}	6.81×10^{17}	4.95×10^{17}	p
4:4	2.17×10^{18}	1.29×10^{18}	0.82×10^{18}	p

The p-type conductivity is greatly enhanced in terms of conductivity and carrier concentration by the dual-acceptor doping with Ag and N. In case of ZnO:(Ag, N) films, the Ag ion occupies the Zn site while N ion is on the O site forming Ag_{Zn} and N_O acceptors. Therefore, the film can easily behave as p-type conduction in achieving shallow acceptor level [4]. From Table 1, the carrier concentration of ZnO:(Ag, N) films significantly increases with the dopant concentration. The highest carrier concentration of 2.176×10^{18} cm^{-3} with a low resistivity of 8.70×10^{-2} Ω cm is obtained for the ZnO:(Ag,N) films at the doping concentration of 4 at%. The growth in grains with the increase of dopant concentration leads to the reduction in grain boundary scattering of charge carriers, thereby increases the carrier concentration of the obtained films [26] and eventually reduces the film resistivity. The lowest resistivity of p-type ZnO:(Ag, N) films prepared by ultrasonic spray pyrolysis reported so far is 56 Ω cm [19]. According to theoretical prediction, among all possible acceptors, N would produce a shallow acceptor level in ZnO [27]. However, Ag theoretically has the lowest transition energy and a shallow acceptor level at 0.3 eV above the valence band maximum [28,29]. Additionally, the formation energy of Ag_{Zn} is theoretically low in O-rich conditions, which could enable the incorporation of high concentrations of dopants and suppress compensating defect formation [28]. To verify the stability and reliability of the electrical properties for the obtained ZnO:(Ag, N) films, the samples have been preserved in an ordinary silica-gel desiccators for a period of 6 months. Table 2 shows the aging effect of carrier concentration with respect to the preservation period. Their p-type conductivities are relatively stable and do not convert to n-type even over 6 months. This fact proves that the ZnO:(Ag, N) films have enhanced stability and conductivity when compared to the mono doped ZnO films reported in literature [19].

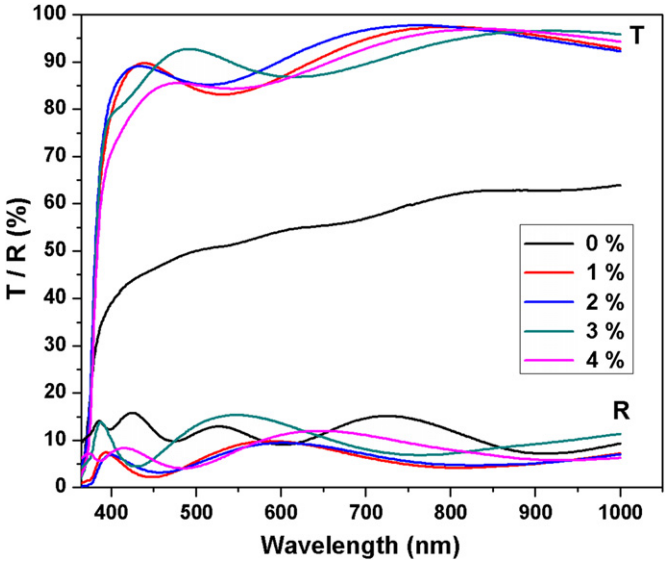

Fig. 6. Transmittance and reflectance spectra of ZnO:(Ag, N) films with various dopant concentrations.

3.4. Optical studies

Fig. 6 represents the optical transmittance and reflectance spectra of ZnO:(Ag, N) thin films with dopant concentration varied from 0 at% to 4 at%. It can be seen that while the undoped ZnO film showed an average transmittance of 52%, all the ZnO:(Ag, N) films exhibited an average transmittance of 89% in the visible region. It is seen that the transmittance is limited by an average reflectance of about 9.5%. The observed decrease in the transmittance at higher dopant concentration may be attributed to the increased scattering of photons by increased surface roughness of the film. The optical transmittance of a film is known to depend strongly on its surface morphology. The RMS surface roughness of the films increases with the increase of dual acceptor doping concentration, which is evident from the AFM result. All the samples showed sharp absorption edge near 375 nm in the UV region. The absorption edge is slightly shifted to longer wavelengths (red shift) with increasing Ag and N concentration.

Fig. 7 illustrates the room temperature PL spectra of the ZnO:(Ag, N) films. The PL spectra consist of UV emission and deep-level emission (DLE). A strong near-band-edge (NBE) ultraviolet emission peak centered at 393 nm (3.16 eV) is related to free exciton–recombination [30]. The weak green emission band related to deep-level emission is observed for all the samples. The peak observed at 484 nm (2.56 eV) is attributed to deep level emission, which originates from the defect emission of oxygen vacancies [31]. It is well known that such DL emission is closely related to intrinsic defects such as Zn interstitials and O vacancies [32], which are believed to act as donor

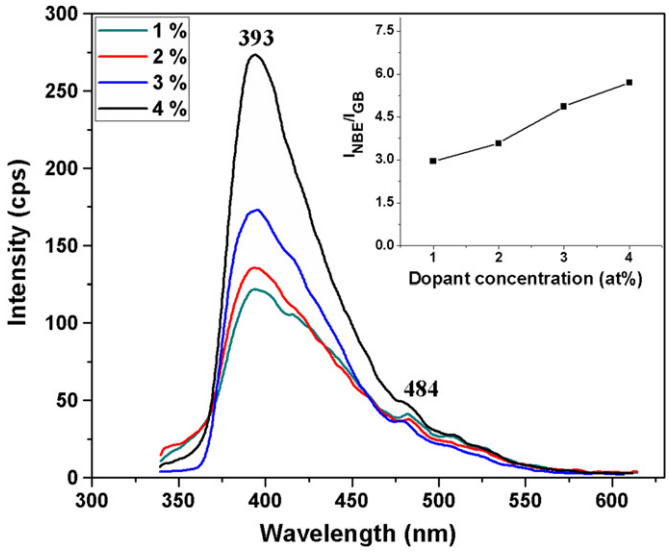

Fig. 7. Photoluminescence spectra of ZnO:(Ag, N) films with different dopant concentrations.

defects. The deep level emission shows a low density of native defects. This also supports the formation of p-type ZnO films by Ag–N dual acceptor doping. The relative intensity ratio between NBE to deep level emission is usually employed to characterize the crystallization [33]. The variation of I_{NBE}/I_{GB} ratio with respect to doping concentration is shown as inset graph in Fig. 7. It has been demonstrated that the ratio of NBE emission to deep level emission of ZnO films depends on the stoichiometry and microstructure of the materials [34]. It should be noted that the increase of I_{NBE}/I_{GB} ratio upon dual acceptor doping implies the increase of crystalline quality. Therefore, these results indicate that the ZnO:(Ag, N) films with high optical quality is obtained at the deposition temperature of 623 K, which is in good agreement with the results of XRD and the Hall-effect measurement.

4. Conclusions

In the present study, the structural, morphological, electrical and optical properties of ZnO:(Ag,N) films deposited by spray pyrolysis (SP) were investigated in detail as a function of dopant concentration. The conductive type of the ZnO:(Ag, N) films showed p-type with increasing Ag and N dopant concentration. The p-type ZnO films with high hole concentration (2.17×10^{18} cm^{-3}) and low resistivity (8.70×10^{-2} Ω cm) were obtained at a dopant concentration of 4 at%. The XRD results revealed a change in the preferential growth from the (100) to (002) direction and an increase in the crystalline quality by the dual acceptor doping of ZnO film. The AFM results illustrated that there is an increase in the surface roughness of the ZnO:(Ag, N) films with the increase of doping concentration. Furthermore, PL spectra of ZnO:(Ag, N) films showed low signal in deep level transition, indicating a low density of native defects. The deposited ZnO:(Ag, N) films showed good transmittance of about 90% in the visible region. The present investigation proves that Ag and N dual acceptor doping is one of the best methods for the preparation of stable p-type ZnO films with acceptable properties for optoelectronic applications.

Acknowledgments

Author M.C.S. Kumar is thankful to the Department of Science and Technology (DST), Govt. of India for the financial support through SERC-Fast Track project for young Scientists.

References

[1] H. Lu, Y. Tu, X. Lin, B. Fang, D. Luo, A. Laaksonen, Effects of laser irradiation on the structure and optical properties of ZnO thin films, Materials Letters 64 (2010) 2072–2075.
[2] Y.J. Chen, Y.Y. Shih, C.H. Ho, J.H. Du, Y.P. Fu, Effect of temperature on lateral growth of ZnO grains grown by MOCVD, Ceramics International 36 (2010) 69–73.
[3] G.H. Lee, Morphology controlled synthesis of ZnO particles through the oxidation of Al–Zn mixture, Ceramics International 36 (2010) 1871–1875.
[4] Z. Yan, Y. Ma, P. Deng, Z. Yu, C. Liu, Z. Song, Ag–N doped ZnO film and its p–n junction fabricated by ion beam assisted deposition, Applied Surface Science 256 (2010) 2289–2292.
[5] S.B. Zhang, S.H. Wei, A. Zunger, Intrinsic n-type versus p-type doping asymmetry and the defect physics of ZnO, Physical Review B 63 (2001) 075205–075212.
[6] X.H. Wanga, B. Yao, C.X. Cong, Z.P. Wei, D.Z. Shen, Z.Z. Zhang, B.H. Li, Y.M. Lu, D.X. Zhao, J.Y. Zhang, X.W. Fan, Hole transport properties of p-type polycrystalline ZnO film using a dual-acceptor doping method with lithium and nitrogen, Thin Solid Films 518 (2010) 3428–3431.
[7] N.H. Erdogan, K. Kara, H. Ozdamar, H. Kavak, R. Esen, H. Karaagac, Structural, optical and electrical properties of N-doped ZnO thin films prepared by thermal oxidation of pulsed filtered cathodic vacuum arc deposited Zn_x N_y films, Journal of Alloys and Compounds 509 (2011) 8922–8926.
[8] Y.J. Zeng, Z.Z. Ye, Y.F. Lu, J.G. Lu, W.Z. Xu, L.P. Zhu, B.H. Zhao, Y. Che, Investigation on ultraviolet photoconductivity in p-type ZnO thin films, Chemical Physics Letters 441 (2007) 115–118.
[9] J. Jiang, L.P. Zhu, J.R. Wang, X.Q. Gu, X.H. Pan, Y.J. Zeng, Z.Z. Ye, Effects of phosphorus doping source temperatures on fabrication and properties of p-type ZnO thin films, Materials Letters 62 (2008) 536–538.
[10] V. Vaithianathana, Y.H. Lee, B.T. Lee, S. Hishita, S. Kim, Doping of As, P and N in laser deposited ZnO films, Journal of Crystal Growth 287 (2006) 85–88.
[11] H.K. Choi, J.H. Park, S.H. Jeong, B.T. Lee, Realization of As-doped p-type ZnO thin films using sputter deposition, Semiconductor Science and Technology 24 (2009) 105003–105007.
[12] X. Pan, Z. Ye, J. Li, X. Gu, Y. Zeng, H. He, L. Zhu, Y. Che, Fabrication of Sb-doped p-type ZnO thin films by pulsed laser deposition, Applied Surface Science 253 (2007) 5067–5069.
[13] M.A. Myers, J.H. Lee, Z. Bi, H. Wang, High quality p-type Ag-doped ZnO thin films achieved under elevated growth temperatures, Journal of Physics: Condensed Matter 24 (2012) 145802–145809.
[14] D. Wang, J. Zhou, G. Liu, Effect of Li-doped concentration on the structure, optical and electrical properties of p-type ZnO thin films prepared by sol–gel method, Journal of Alloys and Compounds 481 (2009) 802–805.

[15] J.G. Lu, Y.Z. Zhang, Z.Z. Ye, L.P. Zhu, L. Wang, B.H. Zhao, Low-resistivity, stable p-type ZnO thin films realized using a Li–N dual-acceptor doping method, Applied Physics Letters 88 (2006) 222114–222117.
[16] X.Y. duan, R.H. yao, Y.J. zhao, The mechanism of Li, N dual-acceptor co-doped p-type ZnO, Applied Physics A 91 (2008) 467–472.
[17] A. Krtschil, A. Dadgar, N. Oleynik, J. Bläsing, A. Diez, A. Krost, Local p-type conductivity in zinc oxide dual-doped with nitrogen and arsenic, Applied Physics Letters 87 (2005) 262105–262107.
[18] Y.Z. Zhang, J.G. Lu, Z.Z. Ye, H.P. He, L.P. Zhu, B.H. Zhao, L. Wang, Effects of growth temperature on Li–N dual doped p-type ZnO thin films prepared by pulsed laser deposition, Applied Surface Science 254 (2008) 1993–1996.
[19] W. Bin, Z. Yue, M. Jiahua, S. Wenbin, Ag–N dual-accept doping for the fabrication of p-type ZnO, Applied Physics A 94 (2009) 715–718.
[20] R. Swapna, M.C. Santhosh Kumar, The role of substrate temperature on the properties of nanocrystalline Mo doped ZnO thin films by spray pyrolysis, Ceramics International 38 (2012) 3875–3883.
[21] C.M. Muiva, T.S. Sathiaraj, K. Maabong, Effect of doping concentration on the properties of aluminium doped zinc oxide thin films prepared by spray pyrolysis for transparent electrode applications, Ceramics International 37 (2011) 555–560.
[22] D. Ma, Z. Ye, L. Wang, J. Huang, B. Zhao, Deposition and characteristics of CdO films with absolutely (200)-preferred orientation, Materials Letters 58 (2003) 128–131.
[23] N. Fujimura, T. Nishihara, S. Goto, J. Xu, T. Ito, Control of preferred orientation for ZnO films: control of self-texture, Journal of Crystal Growth 130 (1993) 269–279.
[24] C.L. Kuo, C.L. Wang, H.H. Ko, W.S. Hwang, K. Chang, W.L. Li, H.H. Huang, Y.H. Chang, M.C. Wang, Synthesis of zinc oxide nanocrystalline powders for cosmetic applications, Ceramics International 36 (2010) 693–698.
[25] H. Nian, S.H. Hahn, K.K. Koo, E.W. Shin, E.J. Kim, Sol–gel derived N-doped ZnO thin films, Materials Letters 63 (2009) 2246–2248.
[26] H.W. Lee, S.P. Lau, Y.G. Wang, K.Y. Tse, H.H. Hng, B.K. Tay, Structural, electrical and optical properties of Al-doped ZnO thin films prepared by filtered cathodic vacuum arc technique, Journal of Crystal Growth 268 (2004) 596–601.
[27] A. Kobayashi, O.F. Sankey, J.D. Dow, Deep energy levels of defects in the wurtzite semiconductors AIN, CdS, CdSe, ZnS, and ZnO, Physical Review B 28 (1983) 946–956.
[28] Y. Yan, S.H. Wei, Doping asymmetry in wide-bandgap semiconductors: origins and solutions, Physica Status Solidi (b) 245 (2008) 641–652.
[29] O. Volnianska, P. Boguslawski, J. Kaczkowski, P. Jakubas, A. Jezierski, E. Kaminska, Theory of doping properties of Ag acceptors in ZnO, Physical Review B 80 (2009) 245212–245219.
[30] Y. Zhao, M. Zhou, Z. Lv, Z. Li, J. Huang, X. Liang, J. Min, Effect of K–N on the structural and optical properties of K–N co-doped ZnO film, Materials Science in Semiconductor Processing 14 (2011) 257–260.
[31] T. Prasada Rao, M.C. Santhosh Kumar, Realization of stable p-type ZnO thin films using Li–N dual acceptors, Journal of Alloys and Compounds 509 (2011) 8676–8682.
[32] B. Lin, Z. Fu, Y. Jia, Green luminescent center in undoped zinc oxide films deposited on silicon substrates, Applied Physics Letters 79 (2001) 943–945.
[33] L.L. Yang, Q.X. Zhao, M. Willander, J.H. Yang, I. Ivanov, Annealing effects on optical properties of low temperature grown ZnO nanorod arrays, Journal of Applied Physics 105 (2009) 053503–053509.
[34] W.J. Wei, B.J. Ming, L.H. Wei, S.J. Chang, Z.J. Ze, H.Li. Zhong, L.Y. Min, D.G. Tong, Enhanced p-type ZnO films through nitrogen and argentum codoping grown by ultrasonic spray pyrolysis, Chinese Physics Letters 25 (2008) 3400–3402.